International Journal of Marine Science and Technology, vol. 2, no. 2, pp. 24–31, 2026
http://doi.org/10.65154/ijmst.39

e-ISSN: 3093-3609
https://i-jmst.vimaru.edu.vn

# Allocation Integrated Sliding Mode Control for Heading Autonomous Underwater Vehicles with Varying Speeds

**Do Khac Tiep*** and **Nguyen Van Tien**

**Abstract:** This paper addresses the challenge of robust heading control for Autonomous Underwater Vehicles (AUVs) operating under variable speed conditions, subject to system nonlinearities, parametric uncertainties, and actuator constraints. We propose a hierarchical control architecture that integrates Sliding Mode Control (SMC) with an optimization-based Control Allocation (CA) scheme. The outer-loop SMC guarantees robustness by computing the required total yaw moment to reject disturbances and track the reference heading. The inner-loop CA then optimally distributes this virtual control effort to individual actuators, explicitly accounting for saturation limits and speed-dependent actuator effectiveness. The performance of the proposed SMC-CA strategy is validated through comprehensive numerical simulations. Results indicate that the system maintains high tracking accuracy and stability across a wide speed range, demonstrating significantly faster transient response and superior disturbance rejection compared to a conventional PID controller in various scenarios, including step changes and abrupt speed variations.

**Keywords:** AUV, control allocation, heading control, nonlinear control, sliding mode control.

## 1. INTRODUCTION

The advancement of autonomous underwater vehicles (AUVs) has revolutionized marine exploration, environmental monitoring, and underwater infrastructure maintenance [1]. However, achieving precise heading control remains a significant challenge due to the highly nonlinear dynamics of the vehicles and the unpredictable nature of the underwater environment [2]. Among various control challenges, the variation in hydrodynamic coefficients at different operating speeds significantly affects the vehicle's maneuverability and stability [3].In the early stages of underwater robotics development, traditional linear control methods were widely adopted. However, as noted by Antonelli [4], these methods often fail to maintain performance when faced with the strong coupling and parametric uncertainties typical of maritime operations. Recent research on the estimation of hydrodynamic coefficients for AUVs emphasizes that the dynamic mesh model must be carefully considered to ensure accuracy [5]. Furthermore, as discussed by Casado and Velasco [6], the design of motion control for specialized configurations, such as X-rudder AUVs, requires sophisticated strategies to handle complex maneuvers.Recent literature reviews by Li and Du [7] highlight that while modern strategies like PID or fuzzy control offer some improvements, they require robust frameworks to handle environmental disturbances effectively. To address these robustness issues, SMC has emerged as a powerful tool. According to Edwards and Spurgeon [8], the primary advantage of SMC is its ability to maintain stability by forcing the system state onto a predefined sliding surface despite modeling uncertainties. Recent applications of SMC in AUV heading stabilization, such as the work by Owais Kamal [9], have demonstrated superior performance in rejecting external noise compared to traditional methods.A critical aspect in AUV control is the management of redundant actuators. Most AUVs are equipped with multiple control surfaces, such as rudders and bow thrusters, which require an efficient distribution of control effort. CA is essential for over-actuated marine vessels to avoid actuator saturation and optimize energy consumption [10]. Furthermore, advanced CA techniques allow for the explicit handling of physical constraints, such as rudder angle limits and rate of change, using sequential quadratic programming [11]. According to the survey by

Manuscript received December 28, 2025; received in revised form February 27, 2026; accepted April 14, 2026; available online June 30, 2026.

Do Khac Tiep and Nguyen Van Tien are with the Faculty of Electrical and Electronic Engineering, Vietnam Maritime University, Haiphong, Vietnam (e-mails: dokhactiep@vimaru.edu.vn and nguyenvantien@vimaru.edu.vn).
* Corresponding author.

**Research article**

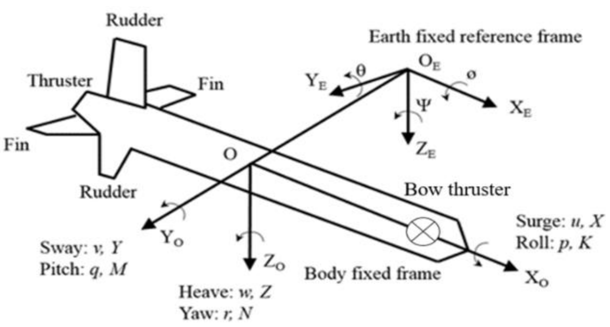


Fig. 1. AUV coordinate system.

Blaha et al. [12], selecting the appropriate optimal control allocation is vital for different vehicle types to achieve desired performance under varying operational envelopes. Recently, Yuan et al. [13] proposed an efficient nonlinear saturation SQP algorithm for control allocation in over-actuated AUVs, combined with a sliding mode observer to compensate for time-varying disturbances and handle typical rudder faults. Despite the individual successes of SMC and CA, there is a lack of integrated research focusing on their combined performance for AUVs operating at variable speeds under environmental disturbances. This paper proposes a hierarchical control architecture to fill this gap. The outer-loop utilizes a robust SMC to compute the required virtual yaw moment $\tau$, while the inner-loop employs an optimization-based CA to distribute this moment among available actuators $u$. By considering the speed-varying hydrodynamic parameters and actuator effectiveness, the proposed strategy ensures stability and high precision across a wide operational range.

The paper is organized as follows: Section 2 details the AUV dynamic model, emphasizing the dependence of hydrodynamic coefficients on speed. Section 3 delves into the design of the SMC controller and the QP control allocation algorithm used. Section 4 presents and analyzes simulation results to evaluate the effectiveness of the proposed method compared to a PID controller. Finally, Section 5 summarizes the main conclusions drawn from the study.

## 2. SYSTEM MODEL

The kinematic model of the AUV describes the relationship between the velocity of the AUV and the change in position and orientation. To construct the kinematic model of an AUV lacking an actuator to perform orientation control, we assume the AUV only moves on a horizontal plane ignoring heave and pitch motions, the kinematic model can be expressed as formula (1).

### 2.1. Mathematical model

We use two main frames of reference to build the mathematical model of the AUV as depicted in Fig. 1. They comprises of global frame $\{E\}$ and body-mounted frame$\{B\}$.

Given an AUV has 6 degrees of freedom. Let $\eta = [x, y, z, \varphi, \theta, \psi]^T$ be the generalized coordinates in the coordinate system $\{E\}$ while $\nu = [u, v, w, p, q, r]^T$ be a velocity vector in the coordinate system $\{B\}$. Remarkably, $(x, y, z)$ are the positions, $(\varphi, \theta, \psi)$ are the roll, pitch, and yaw angles, $(u, v, \mathrm{w})$ are surge, sway, and heave velocities, and $(p, q, r)$ are roll, pitch, and yaw rates.

The relationship between velocity in $\{B\}$ and the derivative of position/posture in $\{E\}$ is given by the transformation matrix $J(n)$ in which $\dot{\eta} = J(\eta)\nu$.

Since the problem focuses on controlling the yaw $\psi$ in the horizontal plane, the most important kinematic equation is: $\dot{\psi} = r$ (assuming small pitch and roll angles)

The general dynamics equation for AUV 6 DOF in reference frame {B} is expressed as

$$M\dot{\nu} + C(\nu)\nu + D(\nu)\nu + g(\eta) = \tau + \tau_{env} \quad (1)$$

where, $M = M_{RB} + M_A$ is inertia matrix combining the rigid body mass/inertia $M_{RB}$ and the additional mass/inertia $M_A$, $C(\nu) = C_{RB}(\nu) + C_A(\nu)$ is Coriolis moment matrix and centrifugal force, $D(\nu)$ is matrix of hydrodynamic drag forces/moments, $g(\eta)$ is restoring force/moment vector due to gravity and buoyancy, $\tau$ is a vector of force/torque from actuators, and $\tau_{\mathrm{env}}$ is perturbation vector from the environment (waves, currents).

To focus on the direction-keeping problem, we consider the equations of motion on the horizontal plane (surge, sway, yaw), assuming the heave, pitch, and roll motions are stabilized by the passive design of the AUV or by other separate controllers and have negligible influence on the yaw. The equation of rotational moment around the $z$-axis, that is the main equation, is expressed as

$$m_{33}\dot{r} + c_{33}(\nu)r + d_{33}(\nu)r = \tau_{\psi} + \tau_{\psi}^{distur} \quad (2)$$

where, $m_{33}$ is component (3,3) of matrix $M$ representing the total inertia around the z-axis (including $I_z$ of the rigid body and the additional inertia $\dot{N}_r$ ), $c_{33}(\nu)$ is component (3,3) of matrix $C(\nu)$ representing the Coriolis effect and centrifugal force on moment yaw, $d_{33}(\nu)$ is component (3,3) of matrix $D(\nu)$ representing the hydrodynamic drag moment for yaw rotation strongly dependent on speed, $\tau_{\psi}$ is the total torque of control around the $z$-axis generated by the actuators, $\tau_{\psi}^{distur}$ is the total disturbance moment acting on the $z$-axis.

### 2.2. Effect of speed on the hydrodynamic coefficient

In AUV dynamics, the hydrodynamic coefficients within the matrices $M$, $C(\nu)$, and $D(\nu)$ are fundamentally dependent on the vehicle's operating speed, $U$ . The total speed through water is defined as $U = \sqrt{u^2 + v^2}$ . Clarifying this relationship is essential for ensuring the robustness of the control laws across a wide operational envelope.

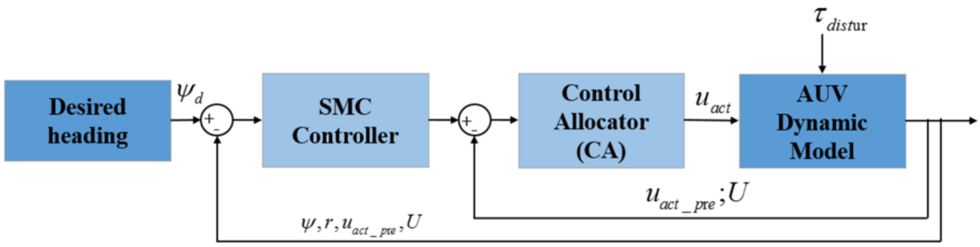


Fig. 2. Structural diagram of the proposed controller.

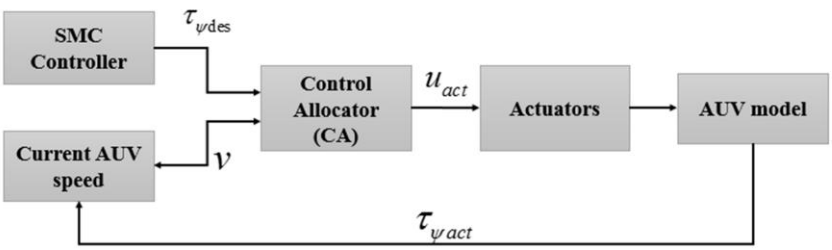


Fig. 3. Structure of control allocation.

The damping forces are the most sensitive components to variations in $U$ due to changes in the Reynolds number and the pressure distribution around the hull. According to the foundational modeling proposed by Fossen [3], the damping matrix can be decomposed into linear and nonlinear (quadratic) components: $D(\nu) = D_{Linear} + D_{Nonlinear}(\nu)$.

For the heading control problem, the yaw damping term $d_{33}(\nu)$ is specifically modeled as a function of $U$ to reflect the increased hydrodynamic resistance at higher velocities: $d_{33}(U) = X_u U + d_{33,quad} |r|$.

Recent experimental studies using horizontal planar motion mechanism tests have confirmed that these coefficients vary nonlinearly as the forward speed increases [5].

While the added mass matrix $M_A$ is often treated as constant in simplified models, it can vary with flow frequency and velocity in practical maneuvers [3]. More importantly, the Coriolis and centrifugal matrix $C(\nu)$ is mathematically constructed from the elements of both the rigid-body mass and the added mass matrices. As a result, any speed-induced variations in the added mass coefficients directly propagate to the Coriolis terms, affecting the overall stability of the yaw motion.

Furthermore, the relationship between the control input u and the resulting forces/moments is governed by the effectiveness matrix $B(U)$. For AUVs utilizing rudders, the lift force generated is proportional to the square of the speed $U^2$. Consequently, the control allocation scheme must account for this time-varying effectiveness to prevent actuator saturation or insufficient control authority at low speeds [10, 12].

### 2.3. Control torque and actuator

The control signal $\tau_\psi$ in equation (2) represents the total virtual control torque around the $z$-axis that the system intends to generate. This torque is produced through the coordinated action of physical actuators, such as the rudder and bow thruster. The relationship between the actual actuator command vector $u = [\delta_r, u_{bow}]^T$ and the resulting yaw moment is described by

$$\tau_\psi = B_\psi(U, \nu, u_{act})u_{act} \tag{3}$$

The explicit dependency of $B_\psi$ on the velocity $U$ is defined by the lift and thrust characteristics of the actuators. For a typical AUV configuration, the matrix is expressed as

$$B_\psi(U) = [b_{rudder}(U) \quad b_{bow}(U)] \tag{4}$$

with $b_{rudder}$ being rudder effectiveness and $b_{bow}$ being bow thruster effectiveness.

The lift force generated by a control surface is proportional to the dynamic pressure, which varies with the square of the flow velocity. The following model is defined as

$$b_{rudder}(U) = \frac{1}{2}\rho L^4 K_\delta U^2 \tag{5}$$

where, $\rho$ is the fluid density, $L$ is the characteristic length, and $K_\delta$ is a dimensionless hydrodynamic coefficient.

Unlike the rudder, the bow thruster is primarily effective at low speeds $U \approx 0$. Its effectiveness decreases as the forward speed increases due to the cross-flow effect that is given by

$$b_{bow}(U) = b_0 \exp(-\alpha U^2) \tag{6}$$

where, $b_0$ is the static thrust coefficient and $\alpha$ is a decay constant.

This time-varying nature of $B_\psi(U)$ necessitates a dynamic CA strategy. The CA module updates $B_\psi(U)$ at each time step based on the measured velocity $U$, ensuring that the optimization-based allocation accurately reflects the current physical capabilities of the actuators. This integration allows the controller to prioritize the bow thruster at low speeds and transition to rudder-dominant control as $U$ increases.

## 3. PROPOSED CONTROLLER DESIGN

To address the problem of controlling the direction of an AUV operating at varying speeds and under the influence of turbulence, this study proposes propose a hierarchical control structure consisting of a SMC in the outer ring and a CA unit (in the inner ring. The SMC ensures stability and calculates the combined control torque, while the CA manages the generation of that torque using actuators (control fins, nose propellers, etc.). The structural diagram of the proposed controller is shown in Fig. 2.

### 3.1. Sliding mode controller

The SMC controller is designed to govern the AUV's yaw kinematics, ensuring that the actual heading angle $\psi$ robustly tracks the desired value $\psi_d$.

The direction error of the control object model is selected as

$$e = \psi - \psi_d \tag{7}$$

To achieve the desired dynamic response and ensure tracking precision for high-order nonlinear maneuvers, a proportional-derivative type sliding surface is defined as

$$s = \dot{e} + \lambda e = (r - r_d) + \lambda(\psi - \psi_d) \tag{8}$$

where, $\lambda > 0$ is a positive design constant determining the convergence rate of the error toward the sliding surface. It is important to note that the control law is designed to handle both constant heading maintenance and time-varying references, where the desired angular velocity $\dot{\psi}_d$ (or $r_d$) is explicitly incorporated into the tracking error dynamics. This formulation ensures that the controller remains applicable to a broad range of AUV missions, including complex trajectory tracking and abrupt setpoint changes as demonstrated in the simulation scenarios.

The SMC control law is designed to ensure that all errors will slide to the selected sliding surface. Consider the yaw kinematic equation from equation (2). Take the derivative of the sliding surface with respect to time and replace $\dot{r}$ from equation (2) into (8), we get

$$\dot{s} = m_{33}^{-1}(\tau_\psi + \tau_\psi^{disturb} - c_{33}(v)r - d_{33}(v,U)r) + \lambda r \tag{9}$$

The SMC control law $\tau_\psi$ usually includes two components: equivalent control $\tau_{eq}$ and switching control $\tau_{sw}$ and is represented by

$$\tau_\psi = \tau_{eq} + \tau_{sw} \tag{10}$$

The $\tau_{eq}$ component is designed to compensate for known dynamic components of the system and maintain $\dot{s} = 0$ if there is no uncertainty and disturbance. Component $\tau_{sw}$ ensure the system converges on the sliding surface ( $s \to 0$ ) and maintain that position despite the influence of modeling uncertainty and perturbation.

Thus, the complete SMC control law is presented by

$$\tau_\psi = m_{33}(\lambda\dot{e} + \ddot{\psi}_d) - c_{33}(v)r - d_{33}(v)r + K\,\mathrm{sign}(s) \tag{11}$$

We use the Lyapunov method to demonstrate the stability of a closed-loop system in the presence of a sliding surface. Consider a Lyapunov candidate

$$V = \frac{1}{2}s^2 \tag{12}$$

It is observed that $V > 0$ for all s $\neq 0$ and $V = 0$ only when $s = 0$. Taking the time derivative of $V$ yields

$$\dot{V} = s\dot{s} \tag{13}$$

From equation (9), the expression for $\dot{s}$ is obtained (after multiplying both sides by $m_{33}$). Therefore,

$$\dot{s} = 1/m_{33}(\tau_\psi + \tau_\psi^{disturb} - c_{33}(v)r - d_{33}(v)r) + m_{33}\lambda r \tag{14}$$

Substituting (11) into (10) yields

$$\dot{V} = s\begin{bmatrix} 1/m_{33}(\tau_\psi + \tau_{env} - c_{33}(v)r \\ -d_{33}(v)r + m_{33}\lambda r) \end{bmatrix} \tag{15}$$

Substituting (8) into (12) and grouping the uncertain components (disturbances) results in

$$\dot{V} = s\Delta - s(K/m_{33})\mathrm{sgn}(s) \tag{16}$$

where, $\Delta$ represents the lumped uncertainties, $\tau_{env}$ denotes environmental disturbances, and $K$ denotes the switching gain.

Let $\mathrm{sgn}(s)$ be the signum function defined as: if $s > 0$ , $\mathrm{sgn}(s) = -1$ and $\mathrm{sgn}(0) = 0$. Consequently, $s\mathrm{sgn}(s) = |s|$.

Thus, the expression for $\dot{V}$ becomes

$$\dot{V} = s\Delta - (K/m_{33})|s| \tag{17}$$

Assume that the total uncertainty and disturbance $\Delta$ is bounded, there exists a positive constant $\Delta_{max}$ such that $|\Delta| \le \Delta_{max}$. Using the inequality $-s\Delta \le |s||\Delta|$, we can determine the upper bound for $\dot{V}$ :

$$\begin{aligned} \dot{V} &\le |s||\Delta| - (K/m_{33})|s| \\ &\le |s|\Delta_{\max} - (K/m_{33})|s| \\ &\le -|s|\left(K/m_{33} - \Delta_{\max}\right) \end{aligned} \tag{18}$$

To ensure that $\dot{V}$ is negative definite, the coefficient of $|s|$ in expression (15) must be positive. This implies that $K$ must be selected sufficiently large such that $K > \Delta_{max}$. If this condition is satisfied, then $\dot{V} < 0$ for all $s \neq 0$ and $\dot{V} = 0$ only when $s = 0$.

### 3.2. Control allocation

The structure of the control allocation system implemented for the AUV heading control is depicted in Fig. 3.

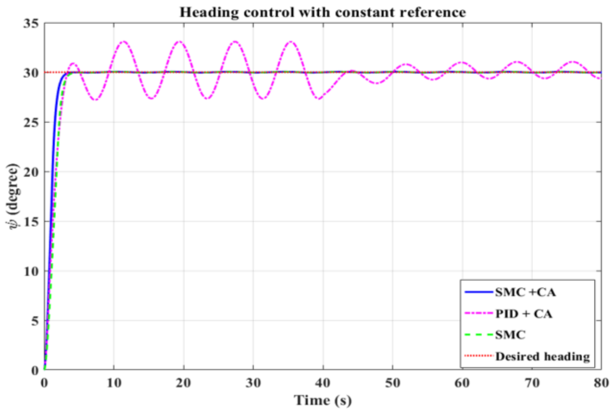

Fig. 4. Heading control with constant reference.

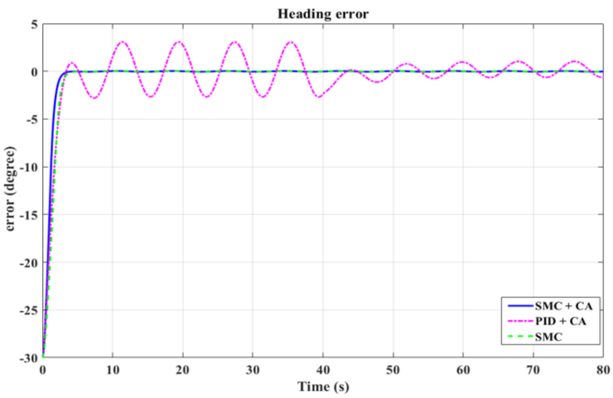

Fig. 5. Heading error with constant reference.

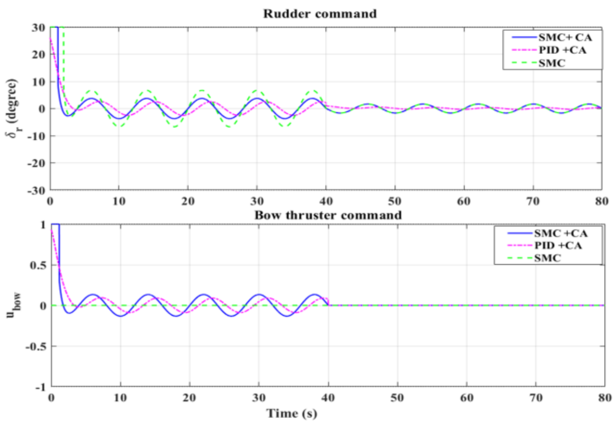

Fig. 6. Rudder and bow thruster.

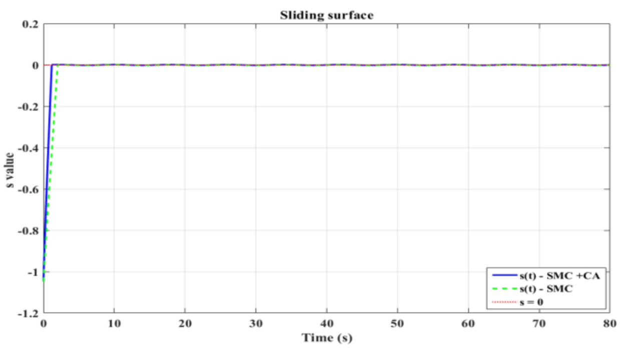

Fig. 7. Sliding surface.

This structure comprises two main control loops: an outer loop utilizing the SMC and an inner loop serving as the CA unit. The task of the SMC is to calculate the desired generalized force and moment vector, denoted as $\tau_\psi$, based on the current state of the AUV. This signal $\tau_\psi$ is then fed into the CA module. Here, the CA plays a pivotal role in distributing this generalized control demand into specific command signals $u_{act}$ for each actuator (e.g., rudder deflection angle, thruster force, etc.). This allocation process accounts for the AUV's current speed (v), as the effectiveness of the actuators is highly dependent on this parameter. Finally, the actuators generate the actual forces and moments $\tau_{\psi actual}$ acting on the AUV to maintain the heading.

Similarly, Liu et al. [15] developed a recursive least squares control allocation method for X-rudder AUVs to handle actuator uncertainty and time-varying control effectiveness, which directly supports the speed-dependent effectiveness matrix used in our work. The block current AUV speed represents the real-time velocity feedback $U$ measured or estimated from the vehicle's navigation sensors. This input is critical for the CA module because the control effectiveness matrix $B_\psi(U)$ must be updated dynamically according to the current speed. Specifically, this feedback allows the QP-based algorithm to adjust the weighting between the rudder and bow thruster, as their physical efficiency varies significantly across different speed regimes.

The relationship between the control command vector $u_{act} \in R^n$ and the actual yaw moment $\tau_{\psi\_actual}$ they produce is described by equation (3). $B(U)$ is the yaw control effectiveness matrix. This matrix contains coefficients describing the efficiency level of each actuator in generating the yaw moment, and these coefficients depend on the AUV speed $U$.

The objective of the CA is to find the command vector $u_{act}$ such that the generated actual yaw moment is as close as possible to the desired yaw moment $\tau_\psi$ from the SMC heading controller: $B_\psi(U).u_{act} \approx \tau\psi$.

**(i) Physical constraint:** The selection of $u_{act}$ cannot be arbitrary but must adhere to the physical limits of the actuators.

**(ii) Amplitude constraint:** Each control command must remain within the allowable operating limits of the corresponding actuator (e.g., maximum rudder angle, maximum/minimum thrust): $u_{\min} \le u_{act} \le u_{\max}$. Where $u_{min}$ and $u_{max}$ are the vectors of lower and upper bounds, respectively.

**(iii) Rate constraint:** To avoid damage or undesirable responses, the rate of change of the control command may also be limited: $\Delta u_{\min} \le u_{act} - u_{act\_prev} \le \Delta u_{\max}$ in which $u_{act\_prev}$ is the control command at the previous time step, and $\Delta u_{min}$ and $\Delta u_{max}$ are the negative and positive rate limits.

To solve the problem of finding $u_{act}$ that satisfies the objective $B_\psi(U).u_{act} \approx \tau\psi$ and the aforementioned constraints, the author utilizes an optimization method based on Quadratic Programming (QP) [11].

The effectiveness of combining SMC with CA has been further validated in recent experimental studies. Ali et al. [14] demonstrated a fault-tolerant control allocation scheme integrated with SMC for a bio-inspired underactuated AUV, achieving robust heading tracking under actuator failures.

QP is a popular and robust choice for CA problems because it allows defining a quadratic objective function to be minimized and directly handles linear constraints. The general QP problem has the form $\min(1/2)x^T Hx + f^T x$ subject to constraints $Ax \le b$ and $A_{eq}x = b_{eq}$ whereas $x$ is the optimization variable vector, $H$ is a positive (semi) definite matrix, $f$ is a vector, $A, A_{eq}$ are matrices, and $b, b_{eq}$ are vectors defining the inequality and equality constraints.

We map the CA problem to QP with optimization variable: $x = u_{act}$. We rypically minimize the squared error between the desired and actual moments, combined with minimizing control energy. The objective function has the form

$$J(u_{act}) = \left\| B_\psi(U)u_{act} - \tau_\psi \right\|_W^2 + \left\| u_{act} \right\|_Q^2 \qquad (19)$$

where, $\left\| B_\psi(U)u_{act} - \tau_\psi \right\|_W^2$ and $\left\| u_{act} \right\|_Q^2$ denote weighted squared norms.

This objective can be rewritten in the standard QP quadratic form

$$J(u_{act}) = u_{act}^H Hu_{act} + f^T u_{act} \qquad (20)$$

where, $H$ and $f$ are obtained from $B_\psi(U)$, $\tau\psi$, while $W$ and $Q$ are weighting matrices.

The CA module uses the QP algorithm to find the optimal control command vector $u_{act}$ at each time step. This process ensures that the yaw moment generated by the actuators tracks the required value $\tau_\psi$ from the SMC controller as closely as possible, while always adhering to their physical limits (amplitude, rate of change) and accounting for the variation in their effectiveness with AUV speed.

## 4. SIMULATION RESULTS

### 4.1. Simulation setup

Simulations were conducted to evaluate the proposed controller against PID and SMC controllers using an AUV with the following parameters: $m$=100 kg, $L$=1.8m, $D$=0.3m, and drag coefficient $C_d$ =0.2. Simulation results for the proposed controller under various scenarios are compared with those of the PID controller. Environmental disturbances acting on the AUV are modeled as a sinusoidal function $\sin(2\pi t/8)$. To validate the performance of the proposed controller, this study simulated the AUV operating in a near-surface condition. The simulation begins with a very low initial speed of 0.4m/s for the first 40 seconds, after which the AUV speed is doubled. The parameters of the controllers used in the simulation are given by

PID: $K_p$=20, $K_i$=1.5, $K_d$=8.

SMC: $\lambda$=50, $k$=3, $\phi$=0.01.

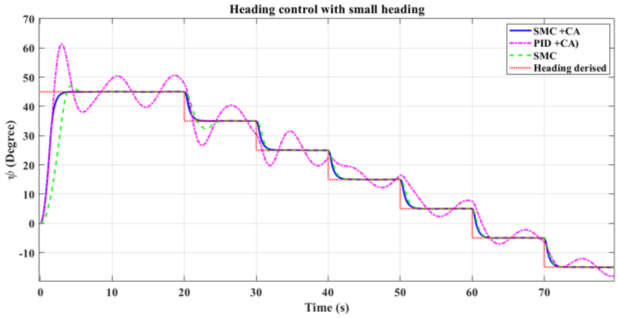


Fig. 8. Heading control with small heading changes.

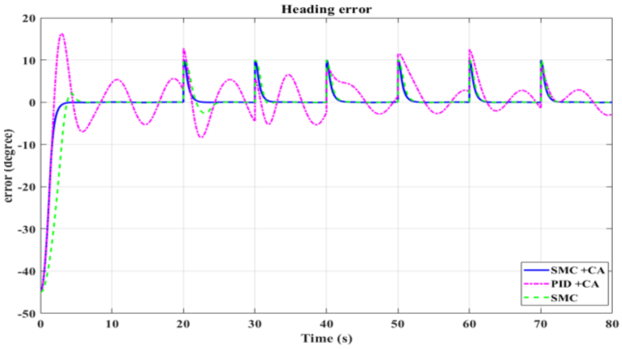


Fig. 9. Heading control with small heading changes.

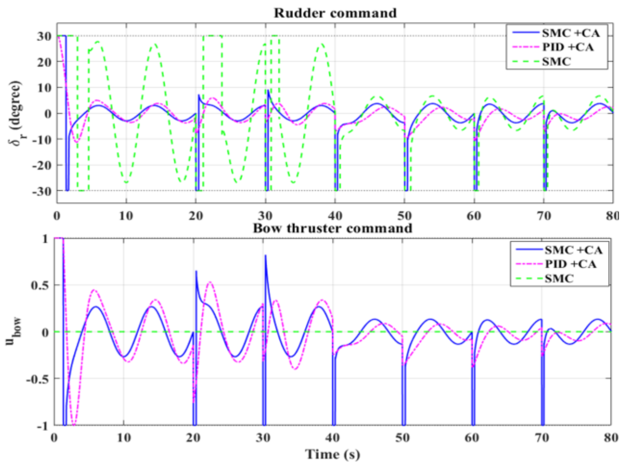


Fig. 10. Rudder and bow thruster.

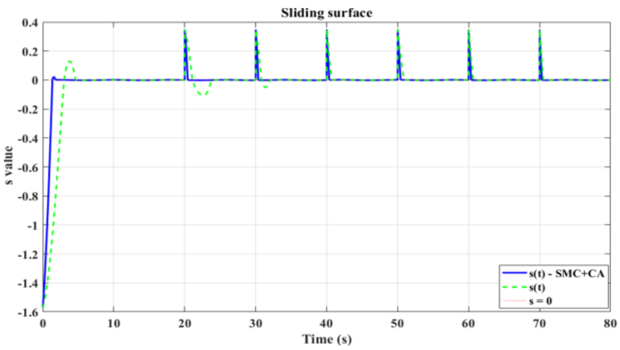


Fig. 11. Sliding surface.

### 4.2. Simulation results

**(i) 1st scenario: Constant heading reference**

Fig. 4 demonstrates the distinct superiority of the SMC combined with CA. The system achieves stability at the 30-degree heading within just 5 seconds with zero

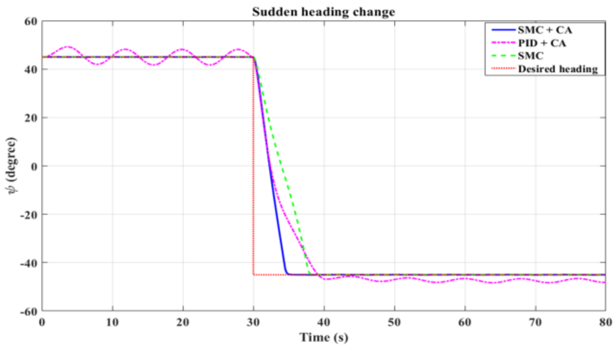


Fig. 12. Heading control with large heading changes.

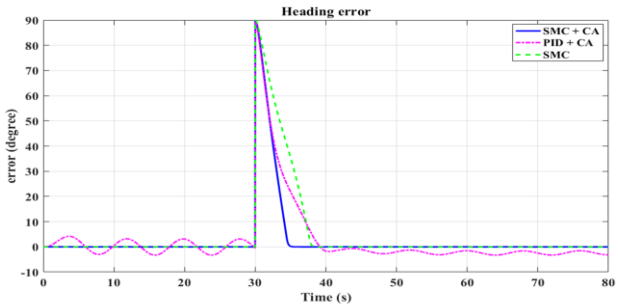


Fig. 13. Heading error with large heading changes.

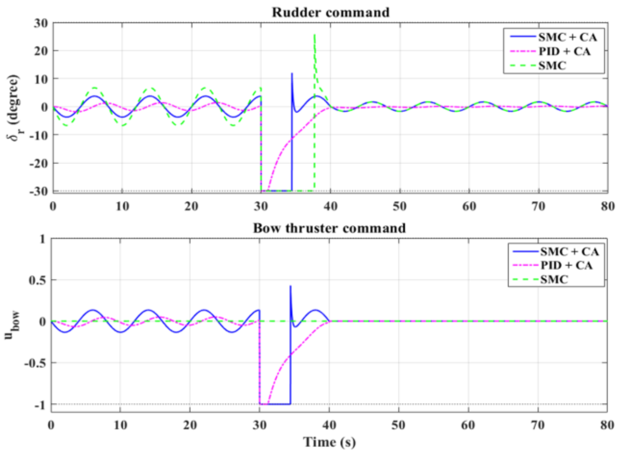


Fig. 14. Rudder and bow thruster.

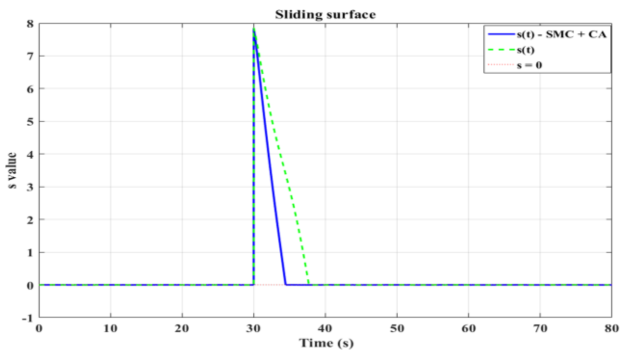


Fig. 15. Sliding surface.

steady-state error. Conversely, the traditional PID controller causes significant, non-decaying oscillations with an initial amplitude of up to $\pm 4$ degrees, revealing the inherent instability of this algorithm in this context. Overall, the SMC controller proves superior in terms of stability, convergence speed, and steady-state precision. The SMC provides an accurate control demand, allowing the CA layer to optimally manage the actuators for smooth and efficient command execution.

Fig. 5 illustrates the heading error. It is evident that the SMC-CA controller completely eliminated the initial error of -30 degrees within 5 seconds, reaching a stable state with zero error. In contrast, the PID controller resulted in large error oscillations of $\pm 4$ degrees and failed to stabilize. This emphasizes that the control allocation layer's ability to optimally execute the robust control command from the SMC is what generates the superior precision and stability.

Fig. 6 highlights the role of CA in intelligently coordinating the rudder and the bow thruster. The SMC-CA controller (blue line) proactively utilized both mechanisms simultaneously to achieve rapid stability. Meanwhile, the controller without CA (green line) abruptly and inefficiently concentrated the entire control effort solely on the rudder. Notably, after 40 seconds when the AUV speed increased, the CA algorithm recognized that the rudder became more effective and subsequently reduced the bow thruster usage to zero, demonstrating the capability for optimal and flexible control resource allocation.

Fig. 7 depicts the sliding surface response of the SMC. As shown, both SMC implementations remain stable by rapidly driving the sliding surface s to 0; however, the method integrated with CA achieves this result more optimally.

**(ii) 2$^{nd}$ scenario: Small heading change**

Fig. 8 demonstrates the performance of the SMC combined with CA in tracking small heading changes. It exhibits superior response capability, accurately tracking the setpoint signal changes without overshoot or oscillation during the heading control process. The role of the CA is emphasized by the smoother heading transitions compared to the non-CA method, attributed to the optimal coordination of actuators during each turn to achieve the most precise response.

In the variable heading tracking scenario, the SMC-CA controller demonstrates the ability to eliminate errors to zero almost instantaneously after each step change, maintaining the sliding surface s stably at 0 (Figs. 9, 11). The role of the CA is best illustrated through the actuator response (Fig. 10), where it flexibly coordinates the rudder and bow thruster to generate smooth responses. This stands in stark contrast to the non-CA method, which continuously and abruptly drives the rudder angle to its saturation limit ($\pm 30$ degrees) to track the signal efficiently. It is thanks to this optimal allocation that the system maintains high stability and precision even during continuous heading changes.

**(iii) 3$^{rd}$ scenario: Sudden heading change**

In the scenario of sudden heading changes where the instantaneous error reaches 90 degrees (Fig. 13), the SMC-CA controller proved its superior performance by completing the turn and stabilizing at the new heading within approximately 8 seconds (Fig. 12). The pivotal role of the CA is most clearly demonstrated in the actuator response (Fig. 14). At the moment of the sudden turn (t = 30s), the CA commanded both the rudder and the bow thruster to operate at maximum saturation (rudder angle at -30 degrees and bow thruster at -1) synchronously to generate the maximum possible torque. This intelligent full-force strategy, distinct from the non-CA method which relies solely on the rudder, is the reason for the system's superior response speed. Even when facing a sudden change that caused the sliding surface s to spike to a value of 8 (Fig. 15), the optimal coordination of the CA ensured the system rapidly stabilized and maintained robustness.

## 5. CONCLUSION

This paper has successfully addressed the complex heading control problem for AUVs operating at variable speeds by proposing a hierarchical control architecture. This architecture synergizes the robustness of the SMC with the optimal allocation capability of the CA module. Simulation results across various scenarios—ranging from constant heading maintenance to sudden course changes—have demonstrated that the proposed SMC-CA method yields superior performance compared to the traditional PID controller. This superiority is evidenced by faster response times, higher precision, and effective oscillation suppression.

The role of the CA module is confirmed as a pivotal factor, facilitating the flexible coordination of actuators, preventing saturation, and optimizing control forces, particularly in high-maneuverability situations. This study provides an effective and highly practical control solution, contributing to enhancing the reliability and autonomy of AUVs under real-world operating conditions.

Future work may focus on integrating more complex environmental disturbance models, such as ocean currents and waves, to further validate and enhance the robustness of the controller.

## ACKNOWLEDGEMENT

This work was supported by the Vietnam Maritime University under Grant DT.25-26.61.

## REFERENCES

[1] R. B.Wynn et al., “Autonomous underwater vehicles: Their past, present and future contributions to the advancement of marine geoscience,” *Marine Geology*, vol. 352, pp. 451-468, 2014.

[2] P. Ridao et al., “Intervention AUVs: The next challenge,” *IFAC-PapersOnLine*, vol. 48, no. 2, pp. 10-17, 2015.

[3] T. I. Fossen, *Handbook of marine craft hydrodynamics and motion control*, John Wiley & Sons, 2011.

[4] G. Antonelli, *Underwater robots*, Springer, 2014.

[5] Y. -H. Lin and Y. -C. Chiu, “The estimation of hydrodynamic coefficients of an autonomous underwater vehicle by comparing a dynamic mesh model with a horizontal planar motion mechanism experiment,” *Ocean Engineering*, vol. 249, pp. 110847, 2022.

[6] M. D. L. Casado and F. J. Velasco, “Design and simulation of X-rudder AUV's motion control,” Ocean Engineering, vol. 137, pp. 204-214, 2017.

[7] D. Li and L. Du, “AUV Trajectory Tracking Models and Control Strategies: A Review,” *Journal of Marine Science* and *Engineering*, vol. 9, no. 9, pp. 1020, 2021.

[8] C. Edwards and S. K. Spurgeon, *Sliding mode control: theory and applications*, CRC Press, 1998.

[9] O. Kamal, “Robust heading stabilization and control for a class of autonomous underwater vehicles using nonlinear state estimators,” 16th *International Bhurban Conference on Applied Sciences and Technology* (IBCAST), 2019.

[10] T. A. Johansen and T. I. Fossen, “Control allocation—A survey,” *Automatica*, vol. 49, no. 5, pp. 1087-1103, 2013.

[11] T. A. Johansen, T. I. Fossen, and S. Berge, “Constrained nonlinear control allocation with singularity avoidance using sequential quadratic programming,” *IEEE Transactions on Control Systems Technology*, vol. 12, no. 1, pp. 211-216, 2004.

[12] T. M. Blaha, E. J. J. Smeur, and B. D. W. Remes, “A survey of optimal control allocation for aerial vehicle control,” *Actuators* , vol. 12, no. 7, pp. 282, 2023.

[13] C. Yuan, C. Shuai, and J. Ma, “An efficient control allocation algorithm for over-actuated AUVs trajectory tracking with fault-tolerant control,” *Ocean Engineering*, vol. 273, pp. 113976, 2023.

[14] W. Remmas and A. Chemori, “Fault-tolerant control allocation for a bio-inspired underactuated AUV in the presence of actuator failures: Design and experiments,” *Ocean Engineering*, vol. 286, pp. 115595, 2023.

[15] W. Wang et al., “Robust trajectory tracking and control allocation of X-rudder AUV with actuator uncertainty,” *Control Engineering Practice*, vol. 136, pp. 105535, 2023.